Vaccine: X 16 (2024) 100443

Contents lists available at ScienceDirect

Vaccine: X

journal homepage: www.elsevier.com/locate/jvacx

Immunogenicity studies of recombinant RBD SARS-CoV-2 as a COVID-19 vaccine candidate produced in *Escherichia coli*

Intan Aghniya Safitri [a,1], Yovin Sugijo [b,1], Fernita Puspasari [b], Fifi Fitriyah Masduki [b,d], Ihsanawati [b], Ernawati Arifin Giri-Rachman [a,d], Aluicia Anita Artarini [c,d], Marselina Irasonia Tan [a,d,*], Dessy Natalia [b,d,*]

[a] *Biology Department, School of Life Science and Technology, Bandung Institute of Technology, Bandung, Indonesia*
[b] *Biochemistry Group, Department of Chemistry, Faculty of Mathematics and Natural Science, Bandung Institute of Technology, Bandung, Indonesia*
[c] *Pharmaceutical Biotechnology Laboratory, Pharmaceutics Department, School of Pharmacy, Bandung Institute of Technology, Bandung, Indonesia*
[d] *Bioscience and Biotechnology Research Centre, Bandung Institute of Technology, Bandung, Indonesia*

ARTICLE INFO

Keywords:
RBD
COVID-19
SARS-CoV-2
Vaccine candidate
Escherichia coli

ABSTRACT

The severe acute respiratory syndrome coronavirus 2 -related global COVID-19 pandemic has been impacting millions of people since its outbreak in 2020. COVID-19 vaccination has proven highly efficient in reducing illness severity and preventing infection-related fatalities. The World Health Organization has granted emergency use approval to multiple, including protein subunit technology-based, COVID-19 vaccines. Foreseeably, additional COVID-19 subunit vaccine development would be essential to meet the accessible and growing demand for effective vaccines, especially for Low-Middle-Income Countries (LMIC). The SARS-CoV-2 spike protein receptor binding domain (RBD), as the primary target for neutralizing antibodies, holds significant potential for future COVID-19 subunit vaccine development. In this study, we developed a recombinant *Escherichia coli*-expressed RBD (rRBD) as a vaccine candidate and evaluated its immunogenicity and preliminary toxicity in BALB/c mice. The rRBD induced humoral immune response from day 7 post-vaccination and, following the booster doses, the IgG levels increased dramatically in mice. Interestingly, our vaccine candidate also significantly induced cellular immune response, indicated by the incrased IFN-ɣ-producing cell numbers. We observed no adverse effect or local reactogenicity either in control or treated mice. Taken together, our discoveries could potentially support efficient and cost-effective vaccine antigen production, from which LMICs could particularly benefit.

Introduction

The novel severe acute respiratory syndrome coronavirus 2 (SARS-CoV-2) emerged in the Chinese city of Wuhan in December 2019, causing symptoms of pneumonia, displaying high transmissibility and rapid global spread [1]. In more than 3 years of the COVID-19 pandemic, by September 2023 more than 770 million cases had been verified, and more than 6.9 million individuals had died as a result of COVID-19 (https://covid19.who.int/).

As of today, the World Health Organization (WHO) has granted emergency use approval to a total of 12 COVID-19 vaccines, with two of them being protein subunit vaccines (source: https://www.bccdc.ca/Health-Info-Site/Documents/COVID-19_vaccine/WHO-EUA-qualified-covid-vaccines.pdf). The global challenge of ensuring vaccine accessibility in less developed regions, compounded by vaccine hesitancy, has hindered global vaccination efforts. Ongoing research and development endeavors are diligently focus on devising innovative vaccines, adjuvants, and immunization strategies to combat such obstacles, underscoring their paramount significance [2].

Consequently, the demand for a cost-effective vaccine production platform enabling swift and inexpensive vaccine antigen generation is immediate and pressing. *Escherichia coli*, a robust protein expression

Abbreviations: AID, Activation-induced deaminase; CAI, Codon Adaptation Index; ELISA, Enzyme-Linked Immunosorbent Assay; IB, Inclusion bodies; LMIC, Low-Middle-Income Countries; RBD, Receptor binding domain; WHO, World Health Organization.

* Corresponding authors.
E-mail addresses: marsel@itb.ac.id (M.I. Tan), dessynatalia@itb.ac.id (D. Natalia).

[1] These authors contributed equally to this work.

https://doi.org/10.1016/j.jvacx.2024.100443
Received 3 July 2023; Received in revised form 16 January 2024; Accepted 18 January 2024
Available online 20 January 2024

host, could be particularly advantegous for such a purpose, offering cost-efficient cultivation possibilities, high expression yields, ease of scalability, and rapid turnaround times. In the vaccine development field, final product affordability is crucial, particularly for Low-Middle-Income Countries (LMIC). The need for an accessible vaccine manufacturing system enabling efficient and affordable vaccine antigen production is thus urging [3].

This stage in subunit protein platform development for vaccine candidates in LMICs marks a pivotal milestone toward obtaining and using such vaccines. Such vaccine candidates serve as blueprints for bioprocessing method establishment for subunit protein platform-based vaccine manufacturing, thereby contributing significantly to ensuring equitable and widespread global access to safe and effective vaccines, enhancing preparedness for potential future pandemics.

Moreover, immunogen selection remains an open question. Whereas most of the approved vaccines use the full-length SARS-CoV-2 spike protein as an immunogen, strong arguments support smaller spike protein fragment-based vaccines, encompassing the receptor binding domain (RBD). RBD-based SARS-CoV-2 vaccines reportedly elicit a higher fraction of neutralizing antibodies (nAbs) than full-length spike protein-based ones, likely due to the entire immune response targeted against the RBD [4,5]. Moreover, high neutralizing titers would be desirable, as nAb levels reportedly strongly correlate with protection [6–8].

Vaccine platform use reportedly improves humoral and cellular immune response against SARS-CoV-2, especially in the case of recombinant RBD (rRBD) as a vaccine candidate [9–11]. Animal studies confirmed that rRBD produced in mammalian cells induced neutralization antibodies [12]. Ai et al [13] and Song et al [14] have demonstrated that complementing the initial two inactivated whole virion vaccine doses with an rRBD booster vaccine is not only safe and highly immunogenic but also significantly enhances the immune response against SARS-CoV-2 and its variants, leading to a robust and stable immunological response. In addition, several FDA-approved subunit vaccines (e.g., Novavax) are available as boosters for those who cannot access or receive FDA-approved messenger RNA bivalent COVID-19 booster vaccines [15].

In this study, we produced rRBD in the *E. coli*, evaluated its immunogenicity, and assessed its preliminary toxicity in BALB/c mice. For immune response enhancement, we administered rRBD together with an aluminum hydroxide adjuvant. Alum is a well-established adjuvant with an over-80-year history of use and the only adjuvant widely approved for human use [16], enhancing immune response strength and efficacy to the co-administered antigen. Therefore, it has been incorporated into numerous licensed vaccines, including those for hepatitis A, hepatitis B, human papillomavirus, diphtheria and tetanus, haemophilus influenza type B, and pneumococcal conjugate vaccines [17,18]. Furthermore, this adjuvant has also been applied in several protein subunit-based COVID-19 vaccine candidates, such as Zifivax (clinical trial 4), EuCorVac-19, GBP510, FINLAY-FR-2 (Soberana 02) (Clinical trial 3), FINLAY-FR1 (Soberana 01), COVAC-1 & COVAC-2 (clinical trial 2), and VAX1 (clinical trial 1) [19]. In this study, we demonstrated that rRBD of SARS-CoV-2 could induce antibody and cellular immune response without causing severe organ-related injury in mice.

Materials and methods

pET16b-RBD construction

We amplified an RBD-encoding DNA fragment from a S1-SARS-CoV-2 synthetic gene- containing plasmid (GenScript, USA), codon optimized for expression in *E. coli*, using the primer pair as follows: catatgCG TGTGCAACCGACCGAAAG and ctcgagtcaGAAGTTCACGCATTTGTTCT TAACC as forward and reverse primer, respectively. First, we cloned the RBD DNA fragment into a pGEM-T vector. Subsequently, we subcloned the RBD DNA fragment, digested with *Nde*I and *Xho*I, from the resulting recombinant pGEMT-RBD into the pET16b expression vector. We then verified the resulting pET16b-RBD using restriction enzymes and nucleotide sequencing analysis.

rRBD Expression, Purification, and refolding

We cultured *E. coli* BL21(DE3)-pET16b-RBD overnight, then inoculated into 100 mL of LB medium (1 % tryptone, 0.5 % yeast extract, and 1 % NaCl) with ampicillin (100 μg/mL) and cultured at 150 rpm shaking and 37 °C until reaching an OD_{600} value of 0.6–0.8. We then supplemented the culture with IPTG at a final concentration of 0.3 mM and incubated for 3 h at 37 °C to induce rRBD expression. Next, we centrifuged the culture at 2935*g* and 4 °C for 10 min to collect the cells.

We resuspended the *E. coli* cell pellet in a solution containing 10 mM Tris-Cl pH 8.0, and 100 mM NaCl. The cells were then lysed using a sonicator at a frequency of 10 kHz for 10 min using the operating conditions of 30–30 s "on" and "off". The lysate was separated by centrifugation at 13,800*g* for 15 min and 4 °C. We then supplemented the rRBD inclusion body-containing cell debris with denaturation buffer (10 mM Tris-Cl pH 8.0; 100 mM NaCl; 8 M urea) at a ratio of 1:5. We then solubilizated the rRBD inclusion bodies by sonicating the suspension for 5 min using the above-described settings and then centrifuged it for 15 min at 13,800*g* and 4 °C to remove the non-solubilized inclusion bodies. We then diluted the denatured rRBD 20 times with unfolding buffer before being applying to the Ni-NTA agarose resin (Qiagen, Germany). The rRBD containing resin was washed with 4-times column volume of unfolding buffer followed by 2 times column volume of low imidazole elution buffer (8 M urea; 10 mM Tris-Cl pH 8.0; 50 mM imidazole; 100 mM NaCl). Finally, we eluted the bound rRBD protein using high imidazole elution buffer (8 M urea; 10 mM Tris-Cl pH 8.0; 300 mM imidazole; 100 mM NaCl). We performed the purification at room temperature.

Next, we refolded the denatured rRBD using the fast-dilution method by adding the refolding buffer (0.05 % sarkosyl; 50 mM Tris-Cl pH 7.4; 1 mM GSH, 500 mM NaCl; 0.1 mM GSSG) to the protein solution at 4 °C. After 30 min of stirring, the refolded rRBD was concentrated using a 10-kDa molecular weight cut-off protein concentrator with a regenerated cellulose membrane (Amicon, USA) at 1878*g* and 4 °C. We then dialyzed the Refolded rRBD with PBS buffer pH 7.4 at 4 °C for 2 h.

Finally, we analyzed the protein profile and concentration using the SDS-PAGE and Bradford methods, respectively. We determined the endotoxin level of rRBD using the LAL Chromogenic Endotoxin Quantitation (Thermoscientific, USA) method following the manufacturer's instruction.

Mouse vaccination with the rRBD

We obtained 6-week-old male and female BALB/c mice of a body weight of 25–30 g (n = 6 for each group) from the animal laboratory of School of Life Science and Technology, Bandung Institute of Technology. The mice were given access to water and feed *ad libitum* and housed with a 12-hours dark-light cycle. We injected the mice intramuscularly with 10-μg rRBD-containing alhydrogel 1.3 % (v/v) or adjuvant alhydrogel 1.3 % with PBS (v/v) as a control on days 1 (first injection), 21 (second injection) and 42 (third injection). On day 21 after the third injection (second booster) or day 63 after the first injection, we sacrificed the animals for organ collection for further preliminary vaccine toxicity study and cytokine-derived T-cell analyses (Fig. 2**A.**). The Research Ethics Committee of Padjadjaran University, Bandung approved animal use in this study (Ethical Clearance No: 501/UN6.KEP/EC/2021).

Prior to mouse vaccination, we observed the rRBD adsorption in alhydrogel adjuvant. For antigen adsorption in the adjuvant, we followed the methods described previously by Jones et al. [20]. We observed that the adjuvant adsorbed 80 % rRBD (Figure S1), fulfilling the minimum WHO requirement [21].

Sample collection

We collected the blood samples by *retro*-orbital bleeding on days 0, 7, 14, 21 and 63 after the first vaccination, incubated them at room temperature for 2 h or until coagulation, then centrifuged at 4 °C and 2800*g* for 10 min. We collected the sera and kept at −80 °C until antibody evaluation.

Mice were sacrificed and their kidney, heart, liver, and spleen were isolated for histopathological study. The kidneys, hearts, and livers were then washed in PBS and weighed. We fixed the organs in Bouin fixative solution and incubated for 24 h. The next day, we rinsed the organs with 70 % ethanol, embedded them into paraffin, sectioned to 7-μm slices using a rotary microtome (American Optical, USA), stained the sections by hematoxylin-eosin for histological examination.

We isolated splenocytes by meshing the spleen aseptically in an RPMI1640 medium (Sigma, USA) with 1 % antibiotic–antimycotic solution (Sigma, USA) and 10 % FBS (Sigma, USA), then filtered the suspension using a 70-μm cell strainer (Corning, USA). Next, we supplemented the suspension with RBC lysis buffer, incubated the mixture for 5 min, and stopped the reaction by adding culture medium, followed by centrifugation at 4 °C and 200*g* for 10 min. After removing the supernatant, we added fresh culture media to the pelleted cell and calculated cell viability using the trypan blue exclusion method in a hemocytometer.

Enzyme-Linked Immunosorbent assay

We analyzed the anti-rRBD antibody levels in mouse sera applying an indirect ELISA method, using PBS for dilution. We used 1-μg/ml rRBD SARS-CoV-2 protein in 50 mM carbonate-bicarbonate buffer pH 9.6 to coat the 96-well ELISA plates (NEST, China), then incubated them overnight at 4 °C. The next day, we rinsed the plate thrice with wash buffer (PBS with 0.1 % (v/v) Tween-20, or PBS-T), blocked with blocking buffer (1 % (w/v) BSA (Millipore, USA) in PBS-T), incubated at room temperature for 1 h, then washed again twice with PBS. We added 50 μL of PBS-diluted mouse serum at a ratio of 1:50 to the well and incubated the plate at room temperature for 2 h, then washed with PBS-T four times. Subsequently, we added 100 μL of 1:10,000 HRP-conjugated goat anti-mouse IgG (AP127P, Millipore USA) or HRP-conjugated goat anti-mouse IgM (NBP1-73694, Novusbio USA) to each well, incubated for 1 h at room temperature, then washed the plate with PBS-T five times, added 50 μL of 3,3′,5,5′-tetramethylbenzidine solution (T0440, Sigma Aldrich, USA) into each well and incubated the plate for 5 min in the dark. The reaction was stopped by adding an equal volume of 1 M H_2SO_4 to the wells, and measured the absorbance at 450 nm using. a microplate reader (iMark, Biorad, USA). We was every sample in triplicates.

In order to observe the binding capacity of rRBD SARS-CoV-2 with specific human IgG, we performed ELISA using convalescent COVID-19 serum and HRP-conjugated goat anti- human IgG (W99003P, Meridian USA) as a secondary antibody. The use of convalescent COVID-19 serum was authorized by Medical Research Ethics Committee of Universitas Jenderal Achmad Yani, Indonesia (No. 164/ KEPK/ FITKES-UNJANI/ VIII/2022).

Cytokine analysis

We performed the cytokine analysis using a cytokine-specific enzyme-linked immunospot (ELISPOT) kit assay (RnDsystems, USA) following the manufacturer's instructions. We cultured the splenocytes and incubated them overnight in an incubator with 5 % CO_2 at 37 °C. We transferred 100 μL of 10^6 splenocytes onto a 96-well PVDF-backed microplate and stimulated with 2 μg/mL of rRBD. We used splenocytes without rRBD and 2 μg/mL concanavalin-A as negative and positive controls, respectively. All these conditions were assayed in triplicate. The splenocytes were then incubated for 24 h in an incubator with 5 % CO_2 at 37 °C. Cells were removed and then the biotinylated anti-IFN-γ/IL-4 was added after washing the plate four times with washing buffer. The plate was incubated overnight at 4 °C. Thereafter, the plate was washed four times with washing buffer, and alkaline phosphatase-conjugated streptavidin was added. The plate was incubated at room temperature for 2 h. Afterward, BCIP/NBT substrates were added to each well and incubated at room temperature for 1 h. The IFN-γ or IL-4 producing cell colonies were observed using a dissecting microscope (Carl Zeiss, Germany) and quantified using ImageJ (https://imagej.nih.gov).

Preliminary toxicity studies

We performed preliminary toxicity studies of vaccine injection in mice using several approaches. After the injection of mice, we observed local reactogenicity on the injection site using the edema and erythema appearance-based Draize scale. We registered the bodyweight every day and body temperature in the ear 1, 2, and 24 h post-injection using an infrared thermometer for animal (OEM, China). After hematoxylin-eosin staining, we examine the histopathology of the kidney, heart, and liver samples using light microscopy (Carl Zeiss, Germany) and scored our observations based on the tissue damage rating as follows: 3 (severe), 2 (moderate), 1 (mild), 0 (normal).

Statistical analysis

We performed the statistical analyses between groups with multiple time points using two-way ANOVA with Tukey's multiple comparison post hoc test. We used unpaired student *t*-test to compare two groups and analyzed nonparametric data using the Mann-Whitney *U* test. We defined statistical significance at P-values of $p < 0.05$.

Results

rRBD production in E. coli BL21(DE3)

We designed the synthetic rRBD encoding gene based on the sequence of the Wuhan-1 variant and codon optimized it for expression in *E. coli*. The 669-bp-size rRBD DNA fragment displayed a high Codon Adaptation Index (CAI) value and GC content of 0.96 and 54.53 %, respectively, which we inserted between the *Nde*I and *Xho*I restriction sites of the pET16b expression vector to produce pET16b-RBD plasmid (Fig. 1**A**), expressing rRBD as an insoluble protein with a molecular mass of 25 kDa (Fig. 1**B**).

We solubilized the inclusion bodies (IB) using 8 M urea and purified the denatured protein using Ni-NTA affinity column chromatography. The unfolded rRBD underwent a refolding process through a rapid dilution technique applying a reduced glutathione (GSH) and oxidized glutathione (GSSG)-containing refolding buffer to facilitate disulfide bond formation and attain the correct rRBD conformation.

rRBD antigenicity evaluation with specific IgG from convalescent COVID-19 serum

We evaluated rRBD antigenicity using ELISA with convalescent COVID-19 serum samples from patients who previously tested positive for SARS-CoV-2 through RT-PCR. We observed that rRBD displayed a specific reactivity against the convalescent COVID-19 serum (Fig. 2).

This result demonstrated that the IgG in the convalescent COVID-19 serum could bind rRBD, suggesting that the rRBD epitope could be recognized by the human IgG paratope in the convalescent COVID-19 serum. Furthermore, we conducted an *in silico* study of rRBD epitopes against B cell receptors using immunoinformatic prediction Bepipred 2.0 on https://tools.iedb.org, seven of which could bind antibodies (Figure S2). Jiang et al. [22] and Li et al.[23] demonstrated that the SARS-CoV-2 RBD epitopes "ATRFAS," "YAWNRKRISN,"

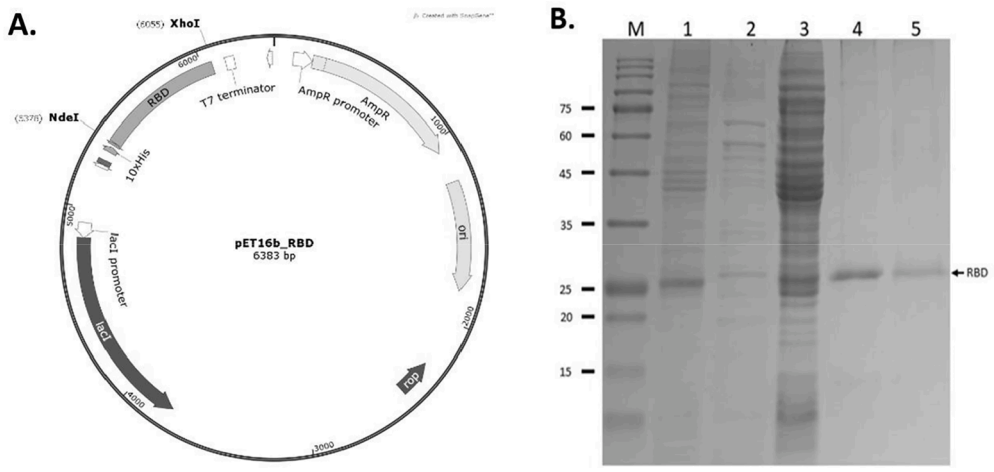

Fig. 1. Plasmid map and rRBD expression profile. A. pET16b-RBD plasmid containing the rRBD gene. B. SDS-PAGE analysis of rRBD production and purification. Lane 1: insoluble fraction (IB) containing rRBD; lane 2: lysate; lane 3: solubilized IB-rRBD; lane 4: NiNTA purified unfolded rRBD; lane 5: refolded rRBD.

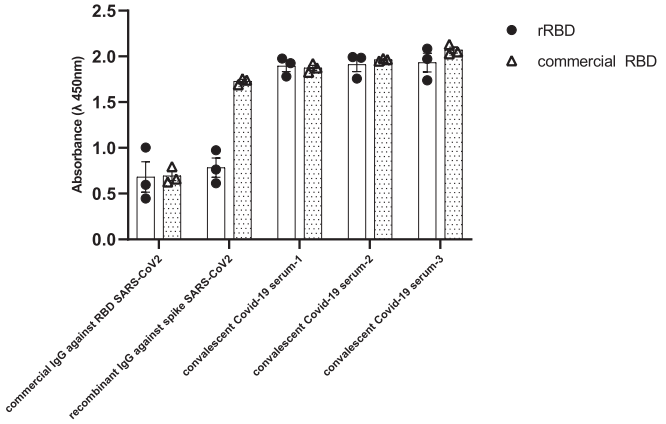

Fig. 2. Comparative antigenicity evaluation of rRBD with commercial RBD using serum from three convalescent COVID-19 patients. Serum was diluted to 1:1000. The data is presented as the mean value of triplicate samples, with error bars indicating the standard error of the means.

"DEVRQIAPGQTGKIADYNYK," "STEIYQAGSTPCNGVE" [22], as well as "VLYNSASFSTFKYGVSP" and "PFERISTEIYQAGSTPC" [23] are dominant and bind immunoglobulins (Ig).

In our study, we acknowledge the limitations of our experiment. We focused solely on investigating antigenicity using our rRBD compared to a commercial rRBD protein. To enhance the reliability and robustness of our research, it is imperative to broaden the spectrum of antigens used in our antigenicity tests. Furthermore, conducting neutralization assays with pseudovirus will help validate and reinforce our findings, resulting in a more comprehensive understanding of the antibody response. Additionally, our forthcoming investigations will delve into the intricate aspects of rRBD folding and explore the specific epitopes responsible for interactions with immunoglobulins, thus deepening our comprehension of these complex mechanisms.

Recombinant RBD elicited a strong humoral immune response in BALB/c mice.

rRBD induced humoral immune response both in male and female BALB/c mice, significantly increasing the IgM and IgG antibodies in the rRBD-Alum group since day 7 post-injection (Fig. 3**B and C**). An rRBD booster dose with intervals of 21 days, dramatically enhanced the IgG levels in the RBD-Alum group (Fig. 3**B and C) with** female mice exhibiting higher IgG antibody levels (Fig. 3**C).**

Female mice (Fig. 3.C) exhibited significantly higher IgG levels compared to male mice (Fig. 3.B) on day 14 ($P = 0.0008$) and day 21 ($P = 0.0002$) after the primary immunization, on day 21 after the first booster ($P = 0.0001$), and on day 21 after the second booster ($P = 0.0051$).

Recombinant RBD induced IFN- γ and IL-4-Secreting cells in spleen

rRBD SARS-CoV-2 successfully induced cellular immunity against RBD SARS-CoV-2. IFN-γ secreting T cell was significantly high in immunized mice (Fig. 4**A**). Therefore, it is possible that rRBD can activate cellular immune response. Moreover, in our study, number of IL-4 secreting splenocytes was higher than the control group (Fig. 4B).

rRBD exhibits no adverse effect

We observed no edema (swelling) or erythema (redness) at the injection site either in female or male mice following vaccination. Moreover, body temperatures remained healthy after vaccination (**Table S1**), with an increase not exceeding 2 °C, indicating that rRBD did not cause fever. Our mouse bodyweight evaluation did not indicate any harmful effect of rRBD either (**Figure S3** and **Table S2**).

Furthermore, we observed no significant differences in the relative organ weight among the mouse groups (**Figure S4**)**.** Taken together, our histopathological study demonstrated that rRBD exhibited no adverse effect on heart, kidneys and liver in mice. Based on the histopathological study of the heart, rRBD did not cause any inflammation, fibrosis, vacuolar, atrophy or hypertrophic myocardium, although we observed few instances of necrosis with a low severity score within the physiological range (**Figure S5**). rRBD did not alter the glomerular and tubular structure in kidneys of the vaccinated mice, although we detected a mild interstitial inflammation especially in the kidney of vaccinated male mice (**Figure S5** and **Table S3**). Finally, we could describe mild inflammation and necrosis in the liver of PBS and vaccinated mice (**Figure S5** and **Table S3**).

Discussion

In this study, we abundantly produced a recombinant RBD (rRBD) SARS-CoV-2 in *E. coli* BL21(DE3), using a cost-effective and scalable production method. rRBD contains two N-linked glycosylation sites, while the absence of glycosylation in rRBD when produced as IB in *E. coli* BL21(DE3), could potentially render it insoluble. However, through a refolding process involving using urea as a denaturing agent, followed by gradual dilution, we have successfully attained the correct rRBD

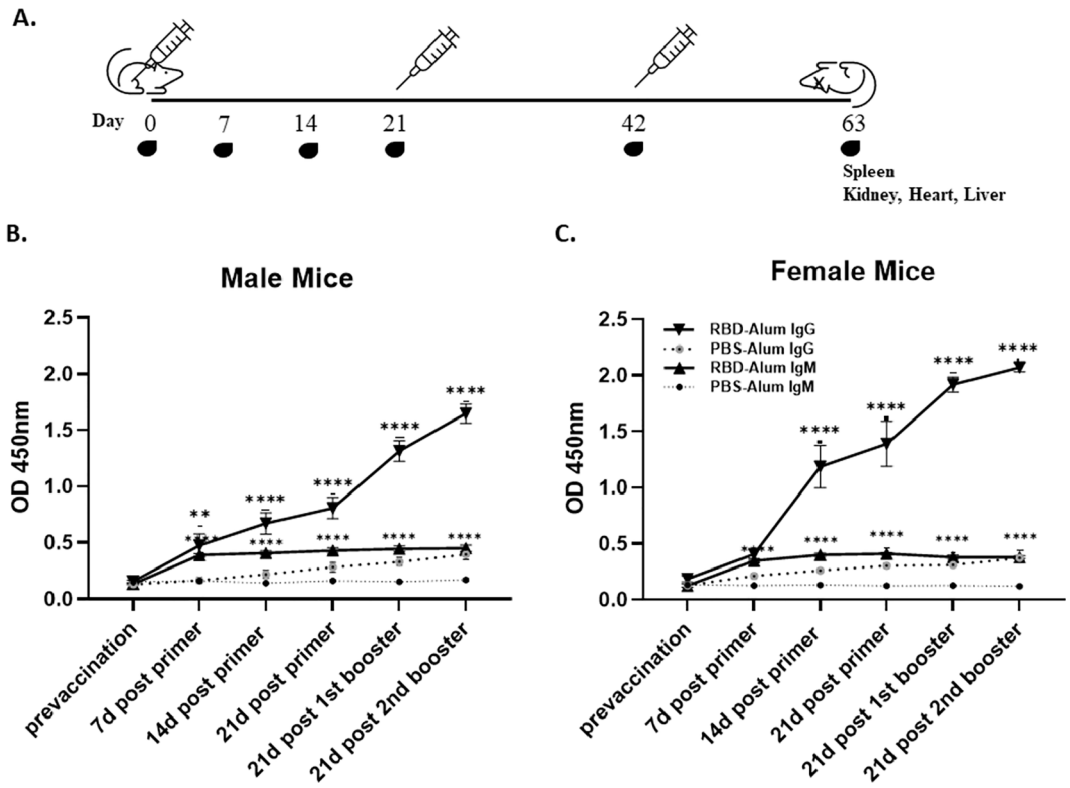

Fig. 3. Mouse immunization with rRBD. A. Immunization and sample collection schedule in BALB/c mice. (B and C) Humoral immune responses against rRBD SARS-CoV-2 in female and male mice (n = 6 for each group) **B and C.** IgG and IgM levels were significantly higher both in male and female mice in rRBD-Alum group than in the PBS-Alum, respectively. $^{**}p < 0.001$, $^{****}p < 0.0001$.

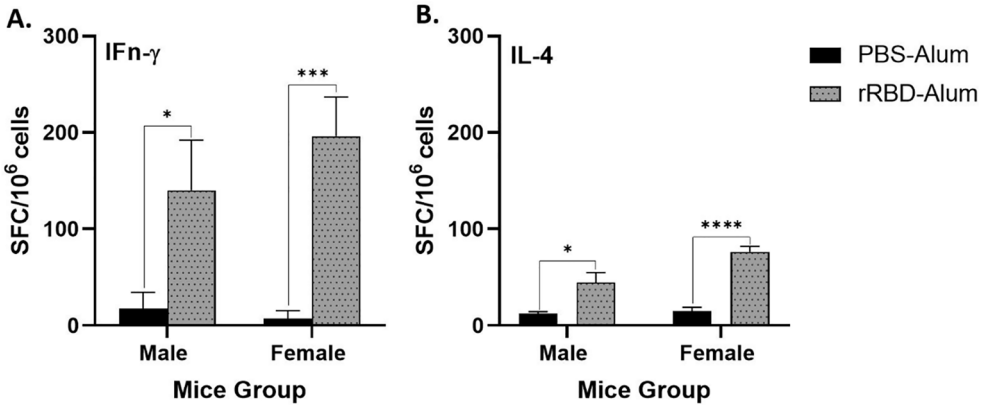

Fig. 4. T-cell responses against rRBD SARS-CoV-2 in mice. A. Male and female mice IFN-γ secreted cells was significantly higher in RBD-Alum group than in PBS-Alum group with $^{*}p < 0.05$ and $^{****}p < 0.001$. **B.** Both female and male mouse group of RBD-Alum displayerd higher number of IL-4 producing cells than PBS-Alum group with statistical significances for male and female of $^{*}p < 0.05$ and $^{****}p < 0.0001$. SFC: Spot Forming Cells.

conformation. Furthermore, our rRBD demonstrated effective interaction with IgG present in a convalescent COVID-19 serum (Fig. 2).

Our immunogenicity study of the obtained adjuvanted rRBD revealed a remarkable humoral immune response in BALB/c mice with pronounced stimulation 21 days post-vaccination (Fig. 3). This finding both reaffirms the robust immunogenicity of adjuvanted rRBD and is also in good agreement with prior results obtained by Du et al. [9] and Yang et al. [10], wherein RBD, when combined with alum, elicited a potent humoral immune response in murine models. In addition, our investigation coincided with a notion put forth by previous studies [9,24,25], suggesting that the 21- and 28-day intervals serve as opportune windows for booster administration. Although our study suggested that rRBD could induce increased antibody production against rRBD, further investigations would be required to determine whether the produced antibodies could neutralize SARS-CoV-2 to confirm rRBD efficacy if developed as a vaccine candidate.

The high humoral immune responses obtained in our study were supported by the *in silico* epitope analysis [26,27] of the SARS-CoV-2 RBD protein. This analysis revealed a plethora of epitopes within rRBD possessing the potential to stimulate B cell production (Table S4). In parallel with the study of Jiang et al. [22], we identified two epitopes, "DEVRQIAPGQTGKIADYNYK" and "STEIYQAGSTPCNGVE," within the SARS-CoV-2 rRBD that exhibited strong interactions with IgG from BALB/c mice. These epitopes notably contained immunodominant peptide sequences, "VRQIAP" and "YQAGSTP," pivotal for eliciting the humoral immune response. Moreover, our work uncovered additional

immunodominant epitopes, "VLYNSASFSTFKYGVSP" and "PFERISTEIYQAGSTPC," reportedly influential in IgG response stimulation in BALB/c mice [23].

Our investigation yielded a remarkable and distinct result, revealing a notable disparity in the immune response against adjuvanted rRBD between female and male mice. Such disparities in immune responses have been observed in vertebrates and could be attributed to inherent hormonal differences between females and males [28]. Hormonal roles, especially that of estrogen, in shaping immune responses has been extensively explored. Building upon this knowledge, our study aligns with that of Pauklin et al. [29], presenting estrogen regulatory influence by upregulating activation-induced deaminase (AID) expression. AID is key in the B-cell class switch recombination and somatic hypermutation, processes critical for humoral immune response adaptability and efficacy.

Further investigation of the adjuvanted SARS-CoV-2 rRBD has yielded a compelling and distinctive outcome, highlighting its ability to induce cellular immunity, a facet that sets study apart. This cellular immune response was characterized by a substantial increase in IFN-γ-secreting T cells, originating from both CD4 + and CD8 + T cell subsets. Sad et al. [30] revealed that CD4 Th1 and CD8-T cells in splenocytes secreted IFN-γ. Intriguingly, our *in silico* study and previous research aligned well [31–33], unveiling 11 epitopes within the SARS-CoV-2 rRBD associated with MHC class I (MHC-I) binding (Table S5). Notably, two of these epitopes, "VSPTKLNDL" and "CGPKKSTNL," exhibited the highest percentile rank in terms of their binding affinity with MHC-I molecules in BALB/c mice. These findings paralleled the observations of Muraoka et al. [34], presenting that the RBD SARS-CoV-2-derived epitope peptide "CGPKKSTNL" specifically induced CD8 + T cell responses in BALB/c mice. RBD also enhanced MHC I expression in dendritic cells compared to the full length of spike protein [35]. The presence of MHC-I epitopes within the adjuvanted rRBD suggests that IFN-γ secretion might be predominantly driven by CD8 + T cells, consistent with the work of Shrivastava et al. [36], demonstrating that mammalian cell-expressed RBD could stimulate CD8 + T cells to secrete IFN-γ. Taken together, these findings underscore the potential of *E. coli*-produced rRBD, as explored in our study, to elicit a robust cellular immune response. In addition, our study aligns with previous ones [37,38] presenting intriguing trends related to glycosylation in RBD-based vaccines. Notably, glycosylation-deleted RBD SARS-CoV-2 mRNA vaccines and those lacking glycan shields on the spike protein have demonstrated heightened CD8 + T cell responses and increased immune levels. These findings further emphasize the unique and promising immunogenicity of *E. coli*-produced rRBD, setting the stage for its potential application in cellular immune-focused vaccine strategy development. Although the adjuvanted rRBD in this study reportedly increases IFN-γ-secreting cells, further studies should, using peptide pools, should aim to ascertain the specific rRBD peptides responsible for inducing cellular immune responses. In addition, despite alum apparently enhancing rRBD immunogenicity, further investigations would be required to determine the most efficient adjuvant for enhancing rRBD immunogenicity.

Our preliminary safety study conducted in Balb/C mice indicated that rRBD SARS-CoV-2 the injection did not result in any edema or erythema. Furthermore, mouse body temperature increased within the range of 0.02–0.18 °C, remaining well within the healthy physiological range [39]. Furthermore, both mouse groups exhibited a steady weight gain of approximately 1.1–1.72 g per week, a pattern that aligns with established norms as confirmed by the standards set by the Jackson Laboratories [40].

rRBD administration did not result in any adverse effects on the heart, liver, or kidneys in mice. We did not observe significant changes were in the relative organ weight or histopathology either. We detected low-level necrosis in all organs with low severity score in both vaccinated and control mice. However, vaccinated male mice exhibited mild interstitial inflammation, particularly in the kidney and liver, of unclear origins, although the observed necrotic and inflammatory changes in the liver could be possibly due to aluminum distress, as previously reported [41,42]. In addition, mild inflammation might be potential caused by rRBD from the SARS-CoV2 spike protein, reportedly exhibiting lipotoxicity potential in liver and kidney cells. A study of Nguyen et al. [43] revealed that the spike protein could interfere with lipid metabolism and the autophagy pathway. Therefore, our results suggest that rRBD is the spike protein segment responsible for this mild inflammation in male mice.

Conclusion

In this study, we produced a recombinant RBD, which successfully elicited both humoral and cellular immune responses in BALB/c mice. rRBD booster dose administration further amplified the IgG levels and promoted IFN-γ- and IL-4-producing cell generation. Importantly, the formulated rRBD demonstrated no toxicity or significant adverse histopathological effects in mouse organs. Taken together, *E. coli*-produced rRBD emerges as a promising SARS-CoV-2 vaccine candidate.

Funding

This work was supported by the Indonesia Endowment Funds for Education (Lembaga Pengelola Dana Pendidikan) - Ministry of Finance and National Research and Innovation Agency (Badan Riset dan Inovasi Nasional) of Indonesia with funding contract No 2/FI/P-KCOVID-19.2B3/X/2020.

Data statement: The data supporting the findings of this study are presented in this manuscript. The corresponding author can provide the raw data upon reasonable request.

Author contributions

IAS performed in vivo and in vitro studies and wrote the manuscript. YS conducted protein preparation and wrote the manuscript. FP carried out plasmid construction. FFM, and Ihs involved in data analysis. AAA, EAGR, MIT and DN contributed in experimental design, data analysis, manuscript writing and revision.

CRediT authorship contribution statement

Intan Aghniya Safitri: Data curation, Investigation, Methodology, Formal analysis. **Yovin Sugijo:** Formal analysis, Investigation, Methodology. **Fernita Puspasari:** Investigation, Methodology. **Fifi Fitriyah Masduki:** Investigation, Project administration. **Ihsanawati:** Investigation, Methodology, Validation, Software. **Ernawati Arifin Giri-Rachman:** Conceptualization, Investigation, Writing – review & editing, Validation. **Aluicia Anita Artarini:** Conceptualization, Investigation, Validation, Writing – review & editing. **Marselina Irasonia Tan:** Conceptualization, Investigation, Supervision, Validation, Writing – original draft, Writing – review & editing. **Dessy Natalia:** Conceptualization, Supervision, Validation, Writing – original draft, Writing – review & editing.

Declaration of competing interest

The authors declare the following financial interests/personal relationships which may be considered as potential competing interests: Dessy Natalia reports equipment, drugs, or supplies was provided by Indonesia Endowment Fund for Education. Marselina Irasonia Tan reports equipment, drugs, or supplies was provided by Indonesia Endowment Fund for Education. Dessy Natalia reports equipment, drugs, or supplies was provided by National Research and Innovation Agency Republic of Indonesia. Marselina Irasonia Tan reports equipment, drugs, or supplies was provided by National Research and Innovation Agency Republic of Indonesia.

Data availability

Data will be made available on request.

Acknowledgments

We express our gratitude to CRODA for providing the Alhydrogel adjuvant, and we extend our thanks to Orca Biotechnology for supplying certain consumables. We also thank Aam Kamal for his support in animal housing, handling, and care; Christian Heryakusuma for his help in English editing, and Adam Darsono for assisting in conducting the ELISA to complete the manuscript revisions.

Appendix A. Supplementary material

Supplementary data to this article can be found online at https://doi.org/10.1016/j.jvacx.2024.100443.

References

[1] Hui DS, I Azhar E, Madani TA, Ntoumi F, Kock R, Dar O, et al. The continuing 2019-nCoV epidemic threat of novel coronaviruses to global health-The latest 2019 novel coronavirus outbreak in Wuhan, China. *Int J Infect Dis* 2020;1(91):264–6. DOI: 10.1016/j.ijid.2020.01.009.
[2] Campbell E, Dobkin J, Osorio LJ, Kolloli A, Ramasamy S, Kumar R, et al. A SARS-CoV-2 Vaccine Designed for Manufacturability Results in Unexpected Potency and Non-Waning Humoral Response. Vaccines 2023;11(4):832. https://doi.org/10.3390/vaccines11040832.
[3] Huang X, Wang X, Zhang J, et al. Escherichia coli-derived virus-like particles in vaccine development. npj Vaccines 2017;2(3). https://doi.org/10.1038/s41541-017-0006-8.
[4] Suthar MS, Zimmerman MG, Kauffman RC, Mantus G, Linderman SL, Hudson WH, et al. Rapid Generation of Neutralizing Antibody Responses in COVID-19 Patients. Cell Rep Med 2020;1:100040. https://doi.org/10.1016/j.xcrm.2020.100040.
[5] Piccoli L, Park YJ, Tortorici MA, Czudnochowski N, Walls AC, Beltramello M, et al. Mapping Neutralizing and Immunodominant Sites on the SARS-CoV-2 Spike Receptor-Binding Domain by Structure-Guided High-Resolution Serology. 1024–1042.e1021 Cell 2020;183. https://doi.org/10.1016/j.cell.2020.09.037.
[6] Gilbert PB, Montefiori DC, McDermott AB, Fong Y, Benkeser D, Deng W, et al. Immune correlates analysis of the mRNA-1273 COVID-19 vaccine efficacy clinical trial. Science 2022;375:43–50. https://doi.org/10.1126/science.abm3425.
[7] Feng S, Phillips DJ, White T, Sayal H, Aley PK, Bibi S, Dold C, Fuskova M, Gilbert SC, Hirsch, I, et al. Correlates of protection against symptomatic and asymptomatic SARS-CoV-2 infection. Nat. Med. 2021, 27, 2032–2040. Feng S, Phillips DJ, White T, Sayal H, Aley PK, Bibi S, Dold C, Fuskova M, Gilbert SC, Hirsch, I, et al. Correlates of protection against symptomatic and asymptomatic SARS-CoV-2 infection. Nat. Med. 2021, 27, 2032–2040. DOI: 10.1038/s41591-021-01540-1.
[8] Sui Y, Bekele Y, Berzofsky JA. Potential SARS-CoV-2 Immune Correlates of Protection in Infection and Vaccine Immunization. Pathogens 2021;10:138. https://doi.org/10.3390/pathogens10020138.
[9] Du Y, Xu Y, Feng J, Hu L, Zhang Y, Zhang B, et al. Intranasal administration of a recombinant RBD vaccine induced protective immunity against SARS-CoV-2 in mouse. Vaccine 2021;39(16):2280–7. https://doi.org/10.1016/j.vaccine.2021.03.006.
[10] Yang J, Wang W, Chen Z, Lu S, Yang F, Bi Z, et al. A vaccine targeting the RBD of the S protein of SARS-CoV-2 induces protective immunity. Nature 2020;586(7830):572–7. https://doi.org/10.1038/s41586-020-2599-8.
[11] Liu Z, Xu W, Xia S, Gu C, Wang X, Wang Q, et al. RBD-Fc-based COVID-19 vaccine candidate induces highly potent SARS-CoV-2 neutralizing antibody response. Signal Transduct Target Ther 2020;5(1). https://doi.org/10.1038/s41392-020-00402-5.
[12] Law JLM, Logan M, Joyce MA, Landi A, Hockman D, Crawford K, et al. SARS-COV-2 recombinant Receptor-Binding-Domain (RBD) induces neutralizing antibodies against variant strains of SARS-CoV-2 and SARS-CoV-1. Vaccine 2021;39(40):5769–79. https://doi.org/10.1016/j.vaccine.2021.08.081.
[13] Ai J, Zhang H, Zhang Q, Zhang Y, Lin K, Fu Z, et al. Recombinant protein subunit vaccine booster following two-dose inactivated vaccines dramatically enhanced anti-RBD responses and neutralizing titers against SARS-CoV-2 and Variants of Concern. Cell Res 2022;32(1):103–6. https://doi.org/10.1038/s41422-021-00590-x.
[14] Song S, Zhou B, Cheng L, Liu W, Fan Q, Ge X, et al. Sequential immunization with SARS-CoV-2 RBD vaccine induces potent and broad neutralization against variants in mice. Virol J 2022;19(1):1–5. https://doi.org/10.1186/s12985-021-01737-3.
[15] Larkin HD. Novavax COVID-19 Vaccine Booster Authorized. JAMA 2022;328(21):2101. https://doi.org/10.1001/jama.2022.20028.
[16] Marrack P, McKee AS, & Munks MW. Towards an understanding of the adjuvant action of aluminium. *Nature Reviews* 2009. *Immunology*, *9*(4), 287–293. https://doi.org/10.1038/nri2510.
[17] Mbow ML, De Gregorio E, Valiante NM, Rappuoli R. New adjuvants for human vaccines. Curr Opin Immunol 2010;22(3):411–6. https://doi.org/10.1016/j.coi.2010.04.004.
[18] Exley C, Siesjö P, Eriksson H. The immunobiology of aluminium adjuvants: how do they really work? Trends Immunol 2010;31(3):103–9. https://doi.org/10.1016/j.it.2009.12.009.
[19] Castrodeza-Sanz J, Sanz-Muñoz I, Eiros JM. Adjuvants for COVID-19 Vaccines. Vaccines 2023;11(5). https://doi.org/10.3390/vaccines11050902.
[20] Jones LS, Peek LJ, Power J, Markham A, Yazzie B, Middaugh CR. Effects of adsorption to aluminum salt adjuvants on the structure and stability of model protein antigens. J Biol Chem 2005;280(14):13406–14. https://doi.org/10.1074/jbc.M50068720.
[21] WHO. Who Manual for the Production and Control of Vaccines World Health Organization. 1977.
[22] Jiang M, Zhang G, Liu H, Ding P, Liu Y, Tian Y, et al. Epitope Profiling Reveals the Critical Antigenic Determinants in SARS-CoV-2 RBD-Based Antigen. Front Immunol 2021;12:1–14. https://doi.org/10.3389/fimmu.2021.707977.
[23] Li S, Duan L, Zhang X, Yang R, Chen L, Chen Z, et al. Immunodominance of epitopes and protection efficacy of RBD antigen are differentially altered by different adjuvants and immune pathways. Research Square 2022. https://doi.org/10.21203/rs.3.rs-1799738/v1.
[24] Tan HX, Juno JA, Lee WS, Barber-Axthelm I, Kelly HG, Wragg KM, et al. Immunogenicity of prime-boost protein subunit vaccine strategies against SARS-CoV-2 in mice and macaques. Nat Commun 2021;12(1):4–13. https://doi.org/10.1038/s41467-021-21665-8.
[25] Zhang N, Ji Q, Liu Z, Tang K, Xie Y, Li K, et al. Effect of Different Adjuvants on Immune Responses Elicited by Protein-Based Subunit Vaccines against SARS-CoV-2 and Its Delta Variant. Viruses 2022;14(3). https://doi.org/10.3390/v14030501.
[26] Jespersen MC, Peters B, Nielsen M, Marcatili P. BepiPred-2.0: improving sequence-based B-cell epitope prediction using conformational epitopes. Nucleic Acids Res 2017;45(W1):W24–9. https://doi.org/10.1093/nar/gkx346.
[27] Vita R, Mahajan S, Overton JA, Dhanda SK, Martini S, Cantrell JR, et al. The Immune Epitope Database (IEDB): 2018 update. Nucleic Acids Res 2019;47(D1):D339–43. https://doi.org/10.1093/nar/gky1006.
[28] Fink AL, Klein SL. The evolution of greater humoral immunity in females than males: implications for vaccine efficacy. Curr Opin Physiol 2018;6:16–20. https://doi.org/10.1016/j.cophys.2018.03.010.
[29] Pauklin S, Sernández IV, Bachmann G, Ramiro AR, Petersen-Mahrt SK. Estrogen directly activates AID transcription and function. J Exp Med 2009;206(1):99–111. https://doi.org/10.1084/jem.20080521.
[30] Sad S, Marcotte R, Mosmann TR. Cytokine-induced differentiation of precursor mouse CD8+ T cells into cytotoxic CD8+ T cells secreting Th1 or Th2 cytokines. Immunity 1995;2(3):271–9. https://doi.org/10.1016/1074-7613(95)90051-9.
[31] Bui H-H, Sidney J, Peters B, Sathiamurthy M, Sinichi A, Purton K-A, et al. Automated generation and evaluation of specific MHC binding predictive tools: ARB matrix applications. Immunogenetics 2005;57(5):304–14. https://doi.org/10.1007/s00251-005-0798-y.
[32] Nielsen M, Lundegaard C, Worning P, Lauemøller SL, Lamberth K, Buus S, et al. Reliable prediction of T-cell epitopes using neural networks with novel sequence representations. Protein Sci 2003;12(5):1007–17. https://doi.org/10.1110/ps.0239403.
[33] Reynisson B, Alvarez B, Paul S, Peters B, Nielsen M. NetMHCpan-4.1 and NetMHCIIpan-4.0: improved predictions of MHC antigen presentation by concurrent motif deconvolution and integration of MS MHC eluted ligand data. *Nucleic Acids Res* 2020 ;2;48(W1):W449–54. DOI: 10.1093/nar/gkaa379.
[34] Muraoka D, Situo D, Sawada SI, Akiyoshi K, Harada N, Ikeda H. Identification of a dominant CD8+ CTL epitope in the SARS-associated coronavirus 2 spike protein. Vaccine 2020;38(49):7697–701. https://doi.org/10.1016/j.vaccine.2020.10.039.
[35] Barreda D, Santiago C, Rodríguez JR, Rodríguez JF, Casasnovas JM, Mérida I, et al. SARS-CoV-2 Spike Protein and Its Receptor Binding Domain Promote a Proinflammatory Activation Profile on Human Dendritic Cells. Cells 2021;10(12). https://doi.org/10.3390/cells10123279.
[36] Shrivastava T, Singh B, Rizvi ZA, Verma R, Goswami S, Vishwakarma P, et al. Comparative Immunomodulatory Evaluation of the Receptor Binding Domain of the SARS-CoV-2 Spike Protein; a Potential Vaccine Candidate Which Imparts Potent Humoral and Th1 Type Immune Response in a Mouse Model. Front Immunol 2021;12:641447. https://doi.org/10.3389/fimmu.2021.641447.
[37] Wu C-Y, Cheng C-W, Kung C-C, Liao K-S, Jan J-T, Ma C, et al. Glycosite-deleted mRNA of SARS-CoV-2 spike protein as a broad-spectrum vaccine. *Proc Natl Acad Sci* 2022;119(9):e2119995119. DOI: 10.1073/pnas.2119995119.
[38] Huang H-Y, Liao H-Y, Chen X, Wang S-W, Cheng C-W, Shahed-Al-Mahmud M, et al. Vaccination with SARS-CoV-2 spike protein lacking glycan shields elicits enhanced protective responses in animal models. *Sci Transl Med* 2022;14(639):eabm0899. DOI: 10.1126/scitranslmed.abm0899.

[39] Lee CT, Zhong L, Mace TA, Repasky EA. Elevation in body temperature to fever range enhances and prolongs subsequent responsiveness of macrophages to endotoxin challenge. PLoS One 2012;7(1). https://doi.org/10.1371/journal.pone.0030077.
[40] The Jackson Laboratory. 2023. Bodyweight information for Balb/cJ. https://www.jax.org/jax-mice-and-services/strain-data-sheet-pages/body-weight-chart-000651.
[41] Muttaqien SE, Mardliyati E, Rahmani S, Pambudi S, Maimunah S, Azki ZI, et al. Intraperitoneal Acute Toxicity of Aluminum Hydroxide Nanoparticle as an Adjuvant Vaccine Candidate in Mice. J Pharmacol Toxicol 2019;15(1):22–35. https://doi.org/10.3923/jpt.2020.22.35.
[42] Fares BH, Al-tememy HAH, Al-Dhalimy AMB. Evaluation of the Toxic Effects of Aluminum Hydroxide Nanoparticles as Adjuvants in Vaccinated Neonatal Mice. Arch Razi Inst 2022;77(1):221–8. https://doi.org/10.22092/ari.2021.356418.1839.
[43] Nguyen V, Zhang Y, Gao C, Cao X, Tian Y, Carver W, et al. The Spike Protein of SARS-CoV-2 Impairs Lipid Metabolism and Increases Susceptibility to Lipotoxicity: Implication for a Role of Nrf2. Cells 2022;11(12). https://doi.org/10.3390/cells11121916.